Journal of Virology®

GENE DELIVERY

A System Based on Novel Parainfluenza Virus PIV5-L for Efficient Gene Delivery of B-Lymphoma Cells

Xiaoqing Liu,[a] Lilan Zheng,[a] Ting Wang,[c] Ying Li,[a] Bingbing Wu,[b] Shujuan Du,[a] Qing Zhu,[a] Caixia Zhu,[a] Yuyan Wang,[a] Rong Zhang,[a] Fang Wei,[b] Qiliang Cai[a,c]

[a]Key Laboratory of Medical Molecular Virology (MOE/NHC/CAMS), Shanghai Institute of Infectious Disease and Biosecurity, and School of Basic Medical Sciences, Shanghai Medical College, Fudan University, Shanghai, People's Republic of China
[b]ShengYushou Center of Cell Biology and Immunology, School of Life Sciences and Biotechnology, Shanghai Jiao Tong University, Shanghai, People's Republic of China
[c]Expert Workstation, Baoji Central Hospital, Baoji, People's Republic of China

Xiaoqing Liu and Lilan Zheng contributed equally to this article. Author order was determined by both alphabetically and in order of increasing seniority.

ABSTRACT Aggressive B-cell lymphoma is one of the most common types of blood malignancy. Robust delivery of genes of interest into target cells, long-term gene expression, and minimal risk of secondary effects are highly desirable for translational medicine including gene therapy and studies on gene function. However, efficient gene delivery into viral or nonviral B-lymphoma cells remains a challenge. Here, we report a strategy for inducing foreign gene expression in B-lymphoma cells by using a vector based on the novel parainfluenza virus PIV5-L (a strain isolated from B cells) that enabled us to study and control the function of a gene product within B-lymphoma cells. Using enhanced green fluorescent protein (eGFP) as a reporter, we successfully rescued PIV5-L and established a one-step system to generate PIV5-L virus-like particles (L-VLPs) with efficient delivery into a broad spectrum of susceptible B-lymphoma cell lines, including Epstein-Barr virus (EBV)- or Kaposi's sarcoma-associated herpesvirus (KSHV)-transformed B-lymphoblastoid cells. Similar to lentiviral vector, the L-VLP highly expressed exogenous genes and remained stable for long periods without obvious negative effects on cell viability. Taken together, these data demonstrate that the PIV5-L-based system provides a potential new strategy for the delivery of desirable genes and the treatment of cancer.

IMPORTANCE B-cell lymphoma is a common aggressive neoplastic disorder of lymphocytes. Delivery of genes of interest into B cells, particularly virus-mediated B-lymphoma cells, is still a challenge. In this study, we report that a system (L-VLP) based on the parainfluenza virus PIV5-L strain isolated from B cells had highly expressed exogenous genes and remained stable without obvious cell toxicity, which provides a potential new strategy for gene delivery and treatment of B-cell cancer.

KEYWORDS PIV5-L, B-cell lymphoma, gene delivery

Lymphocytes exhibit many physiological immune functions based on their lineage and stage of differentiation. Lymphomas arising from these normal lymphoid populations are complex and represent a remarkably diverse group of neoplastic disorders (1, 2). Of these, B-cell lymphomas derived from mature B cells or precursor lymphoid neoplasms, including aggressive non-Hodgkin's lymphomas of diffuse large B-cell lymphoma (DLBCL), Burkitt lymphoma (BL), and primary effusion lymphoma (PEL), are of significant public health concern (2, 3). Epstein-Barr virus (EBV) and Kaposi's sarcoma-associated herpesvirus (KSHV), two human oncogenic gammaherpesviruses, have been shown to be closely associated with several B-cell malignancies, including EBV-positive DLBCL and KSHV-positive PEL, respectively. Among these, EBV-positive DLBCL involves

Editor Rebecca Ellis Dutch, University of Kentucky College of Medicine

Address correspondence to Qiliang Cai, qiliang@fudan.edu.cn, or Fang Wei, fangwei@sjtu.edu.cn.

The authors declare no conflict of interest.

Received 9 February 2022
Accepted 13 March 2022
Published 4 April 2022

clonal B-cell proliferation and often occurs in both elderly and younger patients, predominantly males with immunodeficiency (4). PEL is a B-cell neoplasm derived from the pleural, pericardial, and peritoneal spaces and harbors multiple copies of the KSHV genome, which are required for cell survival. PEL usually occurs in HIV-infected patients, and some cases have also been reported in HIV-negative immunocompromised patients after organ transplantation and in elderly men (5). However, the prognoses of PEL and EBV-DLBCL patients are usually poor, and currently there is no efficient and specific treatment, which requires further investigation. Although several gene delivery technologies, including retrovirus and lentivirus systems, are widely used to study gene functions of interest and for gene therapy (6), the efficiency of delivering exogenous genes into B cells, particularly EBV- or KSHV-positive B-lymphoma cells, is still a challenge and remains to be further improved.

Parainfluenza virus 5 (PIV5), formerly named simian virus 5 (SV5) (7), is a nonsegmented negative-stranded RNA virus (NNSV) of 15,246 nucleotides. It encodes eight proteins, including the nucleocapsid protein (NP), V protein (V), phosphoprotein (P), matrix protein (M), fusion protein (F), small hydrophobic protein (SH), hemagglutinin-neuraminidase (HN), and RNA polymerase large protein (L). Among these, P and V are expressed by a single gene (the V/P gene) that transcribes two independent mRNAs by adding two nontemplated G residues to the P mRNA (8). NP encapsidates genomic RNA to form a helical nucleocapsid structure (ribonucleoprotein, or RNP), which not only serves as a template for transcription and replication by the polymerase complex (consisting of P and L) but can also protect RNA from degradation by nucleases (9). M, HN, and F together are responsible for virus particle production and infection, while M can self-assemble and link the RNP with HN to form the budding site at the cellular membrane to initiate virus particle release (10–12). Although HN or F alone is sufficient to bud particles, the cytoplasmic tail of these two glycoproteins is indispensable for virus assembly and budding (13). When viruses infect host cells, HN, whose RBD (receptor binding domain) performs a sialidases function, binds to and cleaves the sialic acid receptor of the cell membrane and in turn triggers an F conformational change and virus-cell membrane fusion (14).

One promising feature of PIV5 is its ability to infect most mammalian cells without causing cytopathic effects (15). Host cells are persistently infected with PIV5, and there is no potential risk of genetic modification, recombination, or insertion of host cell DNA (16). It has been reported that PIV5 rescued by reverse genetics systems can express green fluorescent protein (GFP) over 20 passages without affecting the replication ability of wild-type virus (17). Therefore, PIV5 could be an ideal delivery vector to express different exogenous proteins. For example, the He group used PIV5 as a vector to generate a vaccine against infection with the fatal Middle East respiratory syndrome coronavirus (MERS-CoV) by expressing MERS-CoV spike protein, which also challenged the limitation of the longest single gene (over 40,00 nucleotides) that can be inserted and expressed within the whole viral genome (18). Recently, the same group also developed a vaccine against SARS-CoV-2 based on the PIV5 vector that achieved promising protective efficacy (19).

In this study, we show a strategy for inducing foreign gene expression in B-lymphoma cells by using a vector based on PIV5-L (a novel strain isolated from B-lymphoma cells in the laboratory). Using enhanced GFP (eGFP) as a reporter, we successfully developed a one-step system to generate PIV5-L virus-like particles (L-VLPs) with more efficient delivery and a broader spectrum of infection of various B lymphoma cell lines, including EBV- or KSHV-infected B-cell lines, than lentiviral vector. These data suggest that the PIV5-L-based system is a new strategy for the delivery of desirable genes and the treatment of cancer.

RESULTS

Isolation and identification of PIV5-L as a novel parainfluenza virus 5 strain. When we performed RNA sequencing of particles from supernatant of B-cell line X,

stored in our laboratory, unexpectedly, 19.2% of the RNA reads matched to parainfluenza virus 5, a rank less than that of only *Homo sapiens* (33.8%). The sequencing data were assembled and compared with the full-length genome sequences of other PIV5 strains published in GenBank. The results revealed that the virus from B-lymphoma cell, named PIV5-L, is a novel parainfluenza virus 5 strain (GenBank accession no. MT160087). Using PIV5-AGS as a reference sequence, we profiled the genome size of PIV5-L as 15,246 bp, containing seven genes, 3′-N-V/P-M-F-SH-HN-L-5′ (Fig. 1A). PIV5-CPI strain has been reported to present a cytopathic effect (20). To look at the similarities to PIV5-L, we aligned the amino acid sequence of eight proteins encoded by PIV5-L and PIV5-CPI. The results showed that PIV5-CPI encodes 6 naturally occurring mutations in the P/V gene (Y26H, V32I, T33I, L50P, L102P, and S157F) that did not take place in PIV5-L. In addition, PIV5-L, not PIV5-CPI, encodes a SH-like protein, which contains 31 amino acid residues, but only the first 12-amino-acid sequence is identical to SH protein due to an open reading frame shift (Fig. 1A, upper).

To confirm the infectivity and cytotoxicity of PIV5-L, various B-lymphoma cell lines were used to infect isolated PIV5-L particles at different multiplicities of infection (MOIs), and we monitored cell viability for 3 days, followed by immunoblot assays with viral V5 antibodies. The results showed that PIV5-L is infectious and can infect a variety of B-lymphoma cell lines, and the viability of most cell lines was not influenced even at an MOI of 30, except BCBL1 was slightly decreased at 3 days postinfection (Fig. 1B).

Generation of PIV5-L and L-VLPs carrying enhanced GFP. To explore whether the novel parainfluenza virus PIV5-L isolated from B-lymphoma cells could be used as a vector for gene delivery into B cells, we performed reverse genetics rescue and constructed a T7 promoter-driven plasmid, pB-PIV5-L-GFP, containing the whole-genome cDNA of PIV5-L with an enhanced GFP gene inserted between HN and L (Fig. 2A) and three support plasmids (pTM1-NP/P/L) to express the viral RNA-dependent RNA polymerase (RdRp) complex, which is important for launching the paramyxovirus rescue process. To efficiently produce progeny viral particles of PIV5-L-GFP, we established a BHK-optT7 stable cell line that expresses codon-optimized T7 polymerase and transfected it with plasmids pB-PIV5-L-GFP and pTM1-NP/P/L. Vero cells were then incubated with the supernatant of the culture medium (Fig. 2B). As expected, at 3 days posttransfection, we observed syncytium formation (a typical cell morphological change after virus infection) in BHK-optT7/PIV5-L-GFP cells (Fig. 2C). The supernatants of culture medium were collected at the fifth day as passage 0 (p0) of PIV5-L-GFP and used to infect Vero cells. Cells with green fluorescence (GFP) were observed at 1 day postinfection, and the ratio of GFP-positive cells to intensity was further enriched at 3 days postinfection (Fig. 2D), indicating that the generation of PIV5-L-GFP to produce progeny viral particles was successfully achieved.

To reduce the safety issue with the use of the virus PIV5-L-GFP as a delivery vector, we also generated a PIV5-L virus-like particle carrying GFP (L-VLP-GFP) with a single-cycle infection that was similar to the lentiviral vector (Fig. 2B, right) (15). Due to the BHK-optT7 stable cell line having hygromycin resistance, we inserted a puromycin resistance (Puro^r) gene into the L-VLP-GFP plasmid as a selectable marker (Fig. 2A, lower). As expected, BHK-optT7 cells with GFP fluorescence were observed at 2 days posttransfection (Fig. 2E). The BHK-optT7 cell line containing L-VLP-GFP (BHK-optT7/L-VLP-GFP) was obtained after puromycin selection. To acquire L-VLP, BHK-optT7/L-VLP-GFP cells were transfected with plasmids expressing M, F, and HN (Fig. 2B, right). At 3 days posttransfection, the supernatants were harvested and used to infect Vero cells. The results showed that GFP fluorescence was observed at 3 days postinfection, while no GFP-positive cells appeared in the supernatant of untransfected BHK-optT7/L-VLP-GFP culture medium as a control (Fig. 2F), indicating that no infectious progeny were produced in BHK-optT7/L-VLP-GFP cells when M, F, and HN were not present. In addition, no GFP-positive Vero cells were observed when incubated with the supernatant from L-VLP-GFP-infected Vero cell culture medium (Fig. 2F, bottom), indicating that L-VLP-GFP-infected cells do not produce infectious progeny particles.

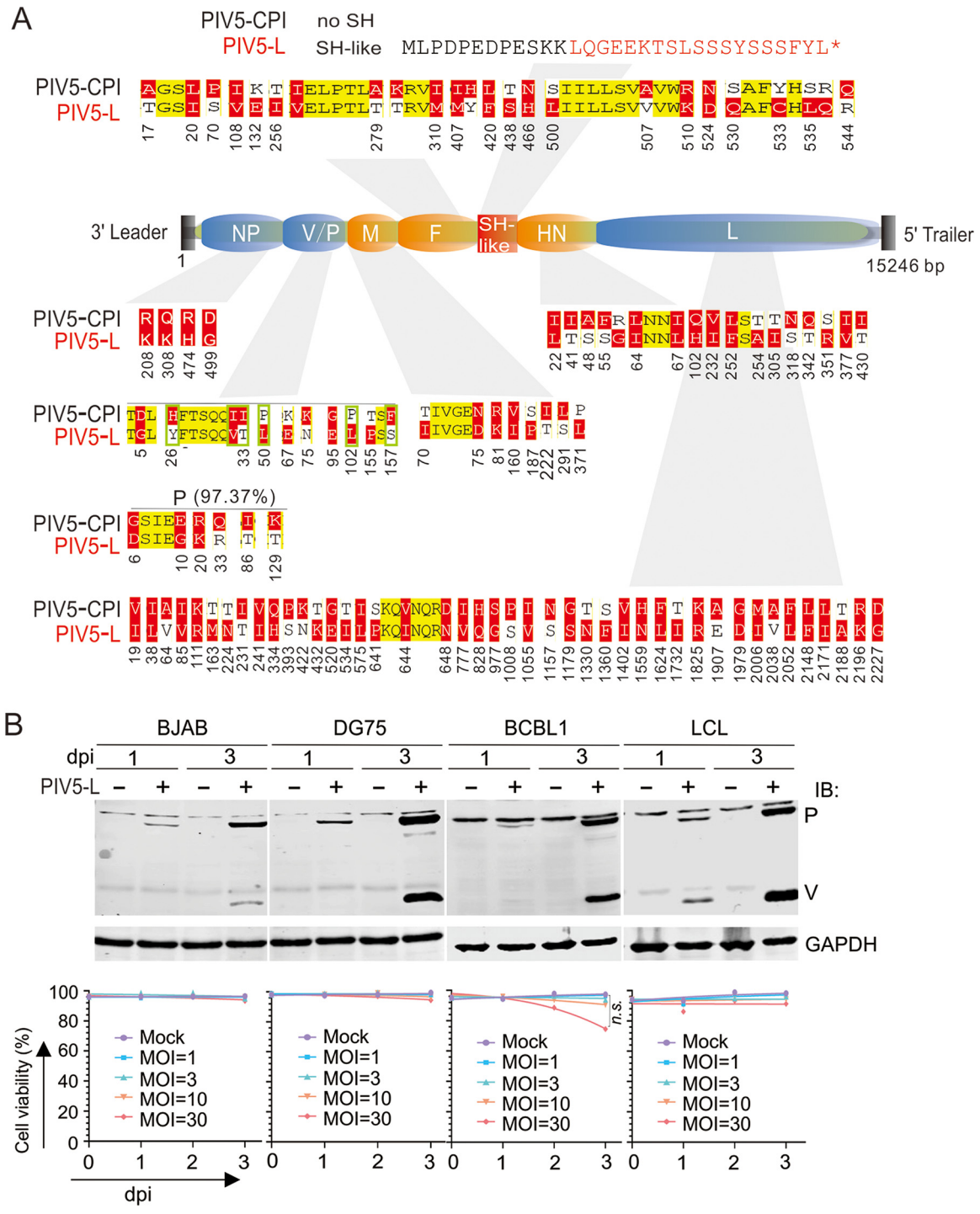

FIG 1 Genome identification of PIV5-L strain from B-lymphoma cells. (A) Amino acid sequence alignment of eight PIV5-L-encoded proteins with PIV5-CPI. Gray shadow indicates each protein for alignment. The amino acid sequence difference is highlighted in red, and identical sequence is in yellow. (B) Cell viability of human B-lymphoma cells infected with PIV5-L at different MOIs was monitored at different time points. (Upper) The efficiency of PIV5-L infection at an MOI of 1 was verified by immunoblotting analysis with V5 antibodies. ns, not significant.

PIV5-L-GFP can infect various B-lymphoma cells efficiently. Since PIV5-L was isolated from a B-lymphoma cell line, we wondered whether rescued PIV5-L-GFP could infect other B-lymphoma cells. To test this possibility, we chose different types of B-lymphoma cells (including EBV-infected, KSHV-infected, or uninfected DG75, BCBL1,

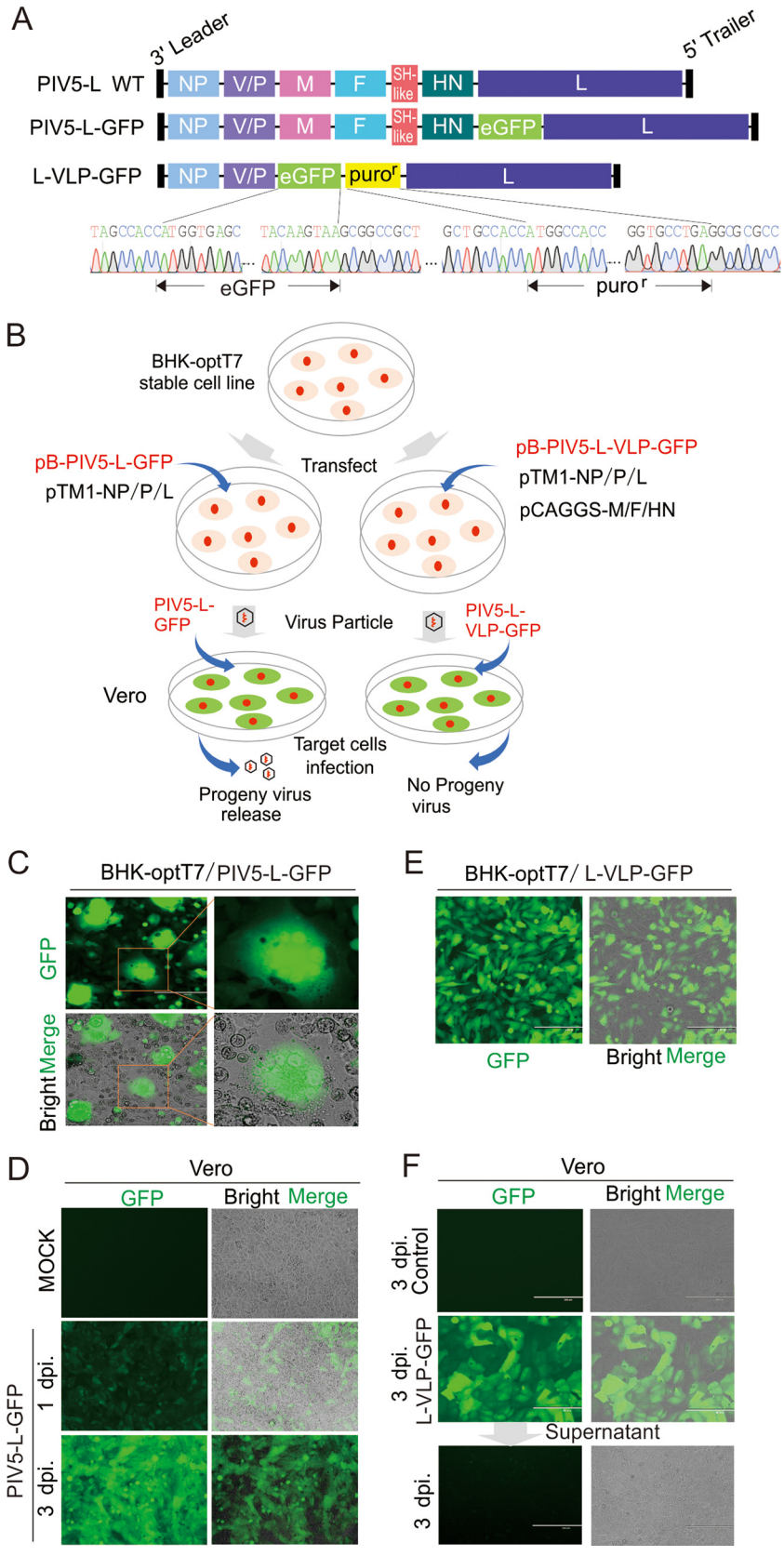

FIG 2 Generation of PIV5-L-GFP and L-VLP-GFP. (A) Schematics of the PIV5-L-WT, PIV5-L-GFP, and L-AVLP-GFP genome sequences. The 3′ leader includes the T7 promoter sequence, and the 5′ trailer includes HDV-Rbz and the T7 terminator sequence (which plays an important role in PIV5 RNA

(Continued on next page)

BC3, B95.8, and LCL cells) to determine the delivery efficiency of PIV5-L by using PIV5-L-GFP. The results showed that at 24 h postinfection, approximately 10% to 20% of the cells in each cell line expressed GFP, and at 48 h, more than 50% of the cells in each cell line expressed GFP, except for the B95.8 cell lines (in which only approximately 20% of cells expressed GFP) (Fig. 3A). The PIV5-L-mediated delivery efficiency of exogenous GFP expression was further confirmed by immunoblotting (Fig. 3B). In addition, evaluation of the cell viability of each cell line after PIV5-L-GFP infection showed that most of the cell lines retained almost the same viability as that of the uninfected group within 3 days postinfection, except for BCBL1, which had a slightly lower viability at 3 days postinfection (Fig. 3C). These data suggest that PIV5-L is a candidate for use as a promising vector to deliver exogenous genes into various B-lymphoma cells.

In addition, growth curves in Vero cells showed that the growth characteristic of PIV5-L-GFP was almost the same as that of PIV5-L. When Vero cells were infected with either PIV5-L or PIV5-L-GFP at an MOI of 0.1 PFU per cell, the titer of both PIV5-L and PIV5-L-GFP reached the highest level, more than 10^7 PFU/mL at 72 h postinfection (Fig. 3D), indicating that GFP gene inserted between HN and L does not affect virus replication.

PIV5-L-VLPs are more suitable than a lentiviral vector for gene delivery into B-lymphoma cells. Lentiviral vectors are conventional and widely used to deliver exogenous genes. To assess whether PIV5-L is a more suitable vector for gene delivery into B-lymphoma cells than a lentiviral vector, we chose different types of B-lymphoma cells, namely, DG75, BC3, and LCL cells, and infected them with the PIV5-L-based vector or lentiviral vector. We then compared the delivery efficiency of PIV5-L-GFP and L-VLP-GFP with lentivirus-GFP side by side. L-VLP-GFP, a single-cycle infectious particle similar to a lentiviral vector, was more comparable than lentivirus-GFP or PIV5-L-GFP for ruling out secondary infection. Notably, unlike that in the lentivirus-GFP-infected group, which rarely exhibited GFP-positive cells among DG75 and LCL cells within 72 h postinfection, the ratio of GFP-positive cells reached nearly 50% in both the PIV5-L-GFP- and L-VLP-GFP-infected group (Fig. 4A and B), and the ratio reached nearly 90% at 72 h postinfection in the PIV5-L-GFP-infected cells. In addition, the efficiency of exogenous GFP gene delivery in the PIV5-L-GFP- or L-VLP-GFP-infected groups was almost higher than that in the lentivirus-GFP-infected group in all tested cell lines, which was further confirmed by the results of immunoblot analysis or infection efficiency at different MOIs (Fig. 4C and D). These results indicate that L-VLP-GFP is more suitable for infection of various B-lymphoma cells than lentivirus-GFP.

To further clarify the effects of L-VLP-GFP as a delivery system on the stability of the long-term expression of exogenous genes and its safety in target cells, we subcultured the DG75, BC3, and LCL cells individually infected with PIV5-L-GFP, L-VLP-GFP, or lentivirus-GFP side by side for a long-term period (7, 14, or 28 days) and then performed immunoblotting and cell viability analysis. The results showed that, similar to that in the lentivirus group, the expression of the GFP gene in both the PIV5-L and L-VLP groups sustained high levels at 28 days without significantly impairing cell viability (Fig. 5A and B), which was confirmed by the consistently higher percentage of GFP-positive cells detected by flow cytometry analysis at different MOIs (Fig. 5C). The viral persistence and

FIG 2 Legend (Continued)
synthesis). NP, nucleoprotein; V/P, phosphoprotein; M, matrix protein; SH-like, small hydrophobic similar protein; F, fusion protein; HN, hemagglutinin-neuraminidase protein; L, RNA-dependent RNA polymerase; puro^r, puromycin resistance protein; eGFP, enhanced green fluorescent protein. The DNA sequence of the portion of L-VLP-GFP with eGFP and puro insertion is shown at the bottom. (B) Streamlined workflow for the generation of PIV5-L-GFP and L-VLP-GFP particles. A BHK cell line stably expressing T7 polymerase was generated and then transfected with different combinations of plasmids as indicated. For PIV5-L-GFP, viruses were harvested at p0 by centrifuging the supernatants, and then Vero cells were infected with PIV5-L-GFP. For L-VLP-GFP, Vero cells were infected with particles directly collected by centrifuging the supernatants. (C) Syncytium formation in BHK-optT7 cells transfected with a combination of PIV5-L-GFP component plasmids. (D) Vero cells left uninfected (mock) or infected with PIV5-L-GFP at 1 day or 3 days postinfection from panel B. (E) BHK-optT7 cells transfected with a combination of L-VLP-GFP component plasmids. (F) Vero cells infected with control or L-VLP-GFP supernatant from panel *E* or supernatant from L-VLP-GFP-infected Vero cells at 3 days postinfection.

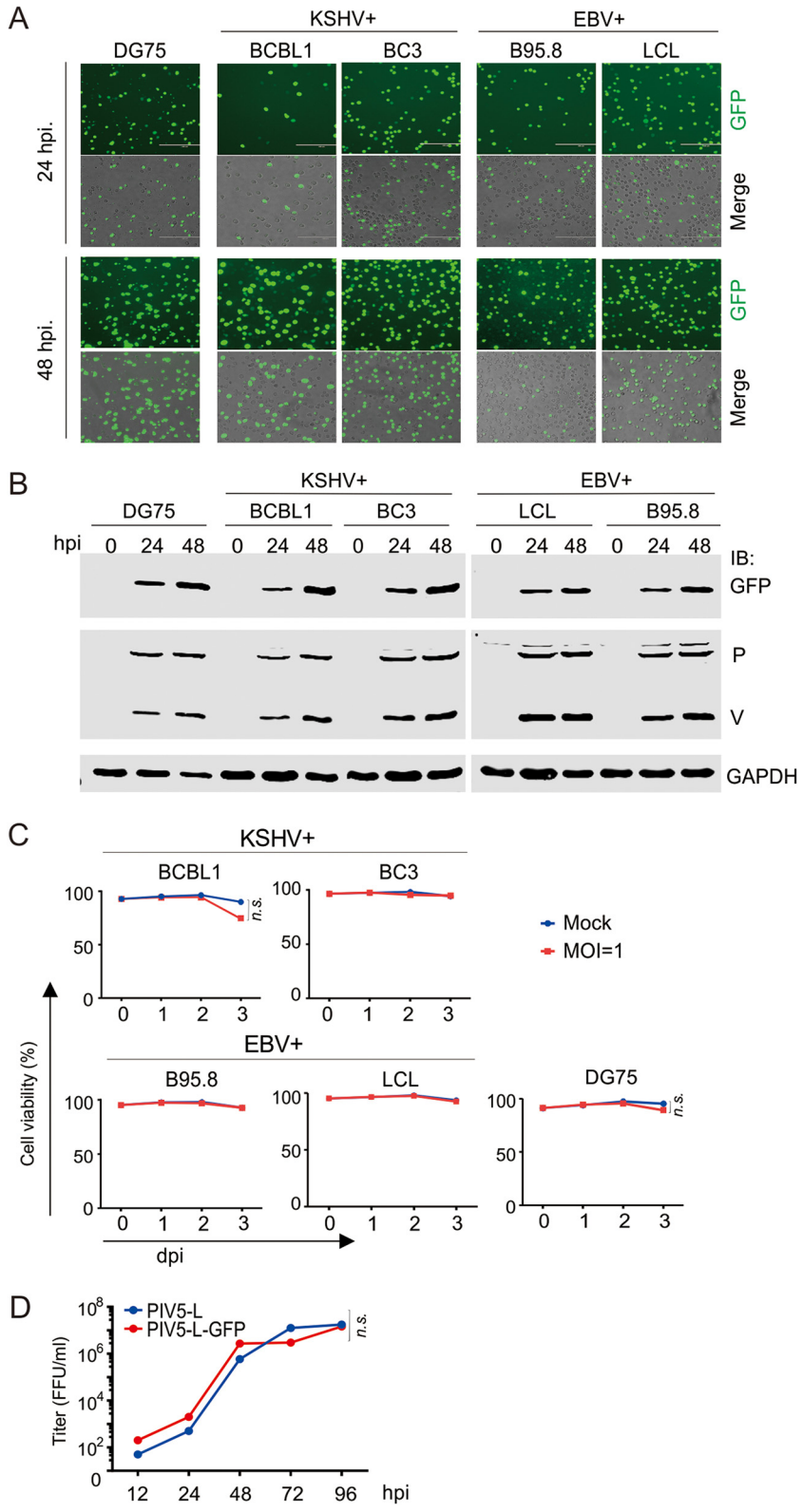

FIG 3 Viral and nonviral B-lymphoma cells are susceptible to PIV5-L infection. (A) High efficiency of PIV5-L infection in various B-lymphoma cells. Different B-lymphoma cell lines, namely, the KSHV and EBV double-negative line DG75, the KSHV-positive lines BCBL1 and BC3, and the EBV-positive lines LCL and B95.8 were individually infected with PIV5-L-GFP at an MOI of 1. Green fluorescence (GFP) images were taken at 24 hpi and 48 hpi. (B) Whole-cell lysates of B-lymphoma cells with PIV5-L-GFP infection from panel A were individually subjected to immunoblot (IB) analysis with the indicated

(Continued on next page)

high cell viability in BCBL1 cells infected with PIV5-L after 65 days of passage observed by Northern blotting and cell viability analysis (Fig. 5D) indicated that the PIV5-L-based vector has enormous advantages and is a promising gene delivery system, especially in B-lymphoma cells.

To further extend the potential application of the PIV5-L-based system, we also compared the delivery efficiency of PIV5-L-GFP and L-VLP-GFP with that of Lenti-GFP in human normal B lymphocytes and primary cancer tissue cells. Interestingly, in healthy human PBMCs, although we observed a few GFP^+ cells under microscopy in both PIV5-L-GFP- and L-VLP-GFP (instead of lentivirus-GFP)-infected groups, $CD19^+$ cells were rarely infected when analyzed by flow cytometry (Fig. 6A). These data indicate that PIV5-L more easily infects B-lymphoma cells than the lentiviral vector but not normal B cells, which could be an advantage for using PIV5-L as a vector for treating B lymphoma *in vivo*. In contrast, in primary breast cancer tissue, a much higher percentage of GFP-positive cells was observed in the PIV5-L-infected group than in the lentivirus-infected group at 48 h postinfection (Fig. 6B) and consistently higher infection efficiency of both PIV5-L-GFP- and L-VLP-GFP than Lenti-GFP in the liver cancer cell lines HepG2 and HepAD38 at different MOIs (Fig. 6C). These results indicate that PIV5-L-based gene delivery is a potential versatile system that enables the expression of genes of interest in various types of cancer cells.

DISCUSSION

In this study, we successfully rescued PIV5-L, which was isolated from a B-lymphoma cell line, and demonstrated that both PIV5-L and its L-VLPs widely infected different types of human B-lymphoma cells and expressed the exogenous genes of interest they carried with high efficiency, as evidenced by the expression of the green fluorescent gene as a reporter. Compared with the lentivirus system, both the PIV5-L and L-VLPs displayed higher efficiency and infected a broader range of B-lymphoma cell types. Although BCBL1 cells presented slight cytotoxicity after PIV5-L infection at approximately 3 to 5 days, the expression of GFP in most PIV5-L-GFP- or L-VLP-GFP-containing B lymphoma cells lasted over a period of 28 days without obvious signs of cytotoxicity, suggesting that the PIV5-L-based system can deliver and sustain the expression of genes of interest over a long time period. On the other hand, distinct from the integration of lentivirus, the property of nonintegration of L-VLP-GFP leading to a gradual reduction of a high level for a long-term period may enhance PIV5-L as a delivery system in balancing effectivity and safety *in vivo*. The observation of different levels of PIV5-L persistence at 28 days or longer postinfection in different types of B-lymphoma cell lines (i.e., DG75, BC3, BCBL1, and LCL) indicated that the effectivity of PIV5-L as a delivery system in different cell types slightly varies, and we need to pay attention to this for use in particular cases in the future.

In addition, since the PIV5-L genome is a negative-sense RNA, unlike the lentiviral genome, it is unlikely to integrate into host chromosomal DNA. The observation that both PIV5-L and its L-VLPs hardly infected normal B lymphocytes *in vitro* further reduces the safety concerns regarding their use as delivery vectors *in vivo*. To simplify the process of PIV5-L and L-VLP production, we established the BHK-optT7 cell line and optimized the ratios of different plasmid components for efficient cotransfection to achieve a high yield rate of viral particles. Moreover, unlike the lentivirus system, which has a redundant infection process, the PIV5-L-based system is much easier to operate and does not require centrifugation at the initial infection.

Regarding the issue of the insertion position of the exogenous gene, it should be considered to balance viral gene stability and exogenous gene expression, because PIV5 has a polarity of transcription, which means the abundance of mRNA decreases with increasing distance from the 3′ promoter due to the disengagement of RNA polymerase and rapid degradation of non-poly(A) mRNAs (21). The common insertion site

FIG 3 Legend (Continued)
antibodies. (C) The cell viability of B-lymphoma cells with or without PIV5-L-GFP infection at an MOI of 1 was monitored at different time points. ns, not significant. (D) Growth curves of PIV5-L, PIV5-L-GFP, and L-VLP-GFP in Vero cells by focus-forming assay. ns, not significant.

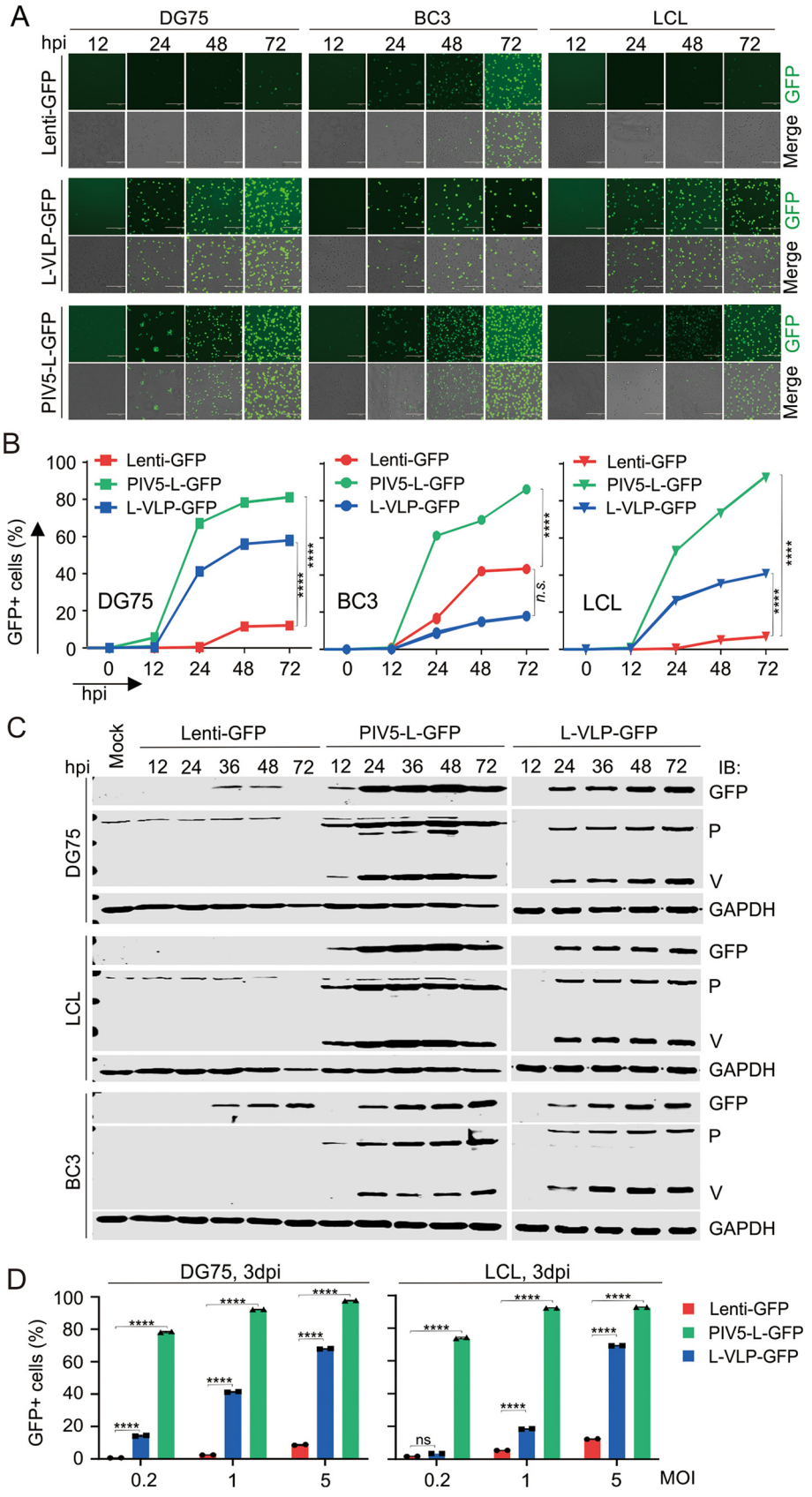

FIG 4 Profiles of different B-lymphoma cells with L-VLP infection. (A) Representative images of DG75, BC3, and LCL B-lymphoma cells infected with Lenti-GFP, L-VLP-GFP, and PIV5-L-GFP at different time

(Continued on next page)

of exogenous genes in PIV5 is located between the SH and HN genes or between the HN and L genes (22). Our PIV5-L strain does not have the traditional SH gene, but the insertion position located between HN and L seemed to work well in our PIV5-L-based system. Recent studies reported that PIV5 could successfully express MERS-CoV spike protein of gene size close to 4 kb (18), indicating that PIV5-L also has the ability to carry the large-sized genes of interests. In addition, the consistently higher percentage and long-term persistence of GFP-positive cells infected by both PIV5-L and L-VLP particles at different MOIs suggest that viral infection and gene expression efficiency are independent of cell proliferation.

To address whether PIV5-L specifically infects B-lymphoma cells and not normal B lymphocytes, we have also tested the infection efficiency of PIV5-L in healthy human peripheral blood mononuclear cells. The rare infection of normal $CD19^+$ B cells with PIV5-L reduces the safety concerns. To reduce the safety issue with the use of the replication virus PIV5 as a delivery vector, several studies have developed single-cycle infection of PIV5-like particles as tools for efficient cargo packaging and delivery by using different strategies (15, 23). In this study, we have also successfully generated a PIV5-L virus-like particle for carrying exogenous gene (L-VLP), which presents higher efficiency or at least efficiency similar to that of the lentiviral vector.

In addition to viral and nonviral B-lymphoma cells, to explore the potential application of PIV5-L in other types of cancer cells, we also performed infection of PIV5-L in both primary breast cancer cells and liver cancer cell lines. The results showed high infection efficiency of both primary breast and liver cancer cells with PIV5-L, indicating that the PIV5-L-based system is a new strategy for the delivery of desirable genes and the treatment of different types of cancer.

In summary, we have demonstrated that the PIV5-L-based system provides a potential new strategy that is versatile and efficient and can easily deliver desirable genes and treat B-lymphoma and other types of primary cancer.

MATERIALS AND METHODS

Cell cultures. BHK-optT7, Vero, and primary breast cells were cultured in 10% fetal bovine serum (FBS)–Dulbecco's modified Eagle medium (DMEM) (Gibco) with 1% penicillin, gentamicin, and streptomycin (Gibco-BRL). B-lymphoma cell lines HepG2 and HepAD38 and human PBMCs were cultured in 10% FBS–RPMI 1640 (HyClone) medium with 1% penicillin, gentamicin, and streptomycin (Gibco-BRL). All cell lines were incubated at 37°C in a humidified environmental incubator with 5% CO_2.

Reagents and antibodies. Antibodies to V5 (2B7A9 [Proteintech] for Western blotting; D3H8Q [CST] for flow cytometry), GFP (F56-6A1; Santa Cruz), and glyceraldehyde-3-phosphate dehydrogenase (GAPDH) (G8140-01; US Biological) were used.

Viral genome sequencing and analyses. The supernatant of B-cell line X culture medium was filtered through a 0.45-μm filter and ultracentrifuged at 290,000 $\times$ *g* for 2 h. Pellets were suspended in 100 μL of phosphate-buffered saline (PBS), and the RNA from the suspension was isolated using TRIzol reagent according to the manufacturer's instructions (Invitrogen). The extracted RNA was submitted to OE Biotech (Shanghai, China) for high-throughput sequencing in an Illumina sequencing system based on the transcriptome *de novo* sequencing platform. The obtained viral contigs were analyzed and annotated by the MG-RAST server. The cutoff for the annotation was a maximum *E* value of 1e−10, 80% minimum percentage identity, and 35 bp for minimum alignment length. The viral genomic sequences were obtained by reverse transcription-PCR (RT-PCR) using primers based on the parainfluenza virus 5-associated contigs obtained by high-throughput sequencing.

Plasmid construction. For construction of pB-PIV5-L-GFP, the full-length virus genomic cDNA was amplified from viral RNA by reverse transcription (AT301; Transgene) and PCR (primer star mix; TaKaRa). The complete cDNA of the 15,246-nucleotide PIV5-L genome was divided into 6 fragments using 6 pairs of primers, and then we inserted these fragments into pBluScriptIISK(+) by an in-fusion cloning technique (D7010S; Beyotime). Three support plasmids, pTM1-NP, pTM1-P, and pTM1-L, were generated by amplification from full-length cDNA, and then we ligated PCR product into pTM1 plasmid, which contained T7 promoter and internal ribosomal entry site elements. pB-PIV5-L-VLP-GFP was constructed by

FIG 4 Legend (Continued)
points (MOI, 1). The green fluorescence (GFP) and bright merged images are shown as indicated. (B) The percentage of GFP-positive B-lymphoma cells after viral infection from panel A was quantified by flow cytometry analysis. The statistical analysis at 3 days postinfection is shown. (C) Immunoblot analysis of B-lymphoma cells after viral infection from panel A was performed with the indicated antibodies. (D) The percentage of GFP-positive B-lymphoma cells with viral infection at different MOIs at 3 days postinfection was quantified by flow cytometry analysis. ****, $P < 0.0001$. ns, not significant.

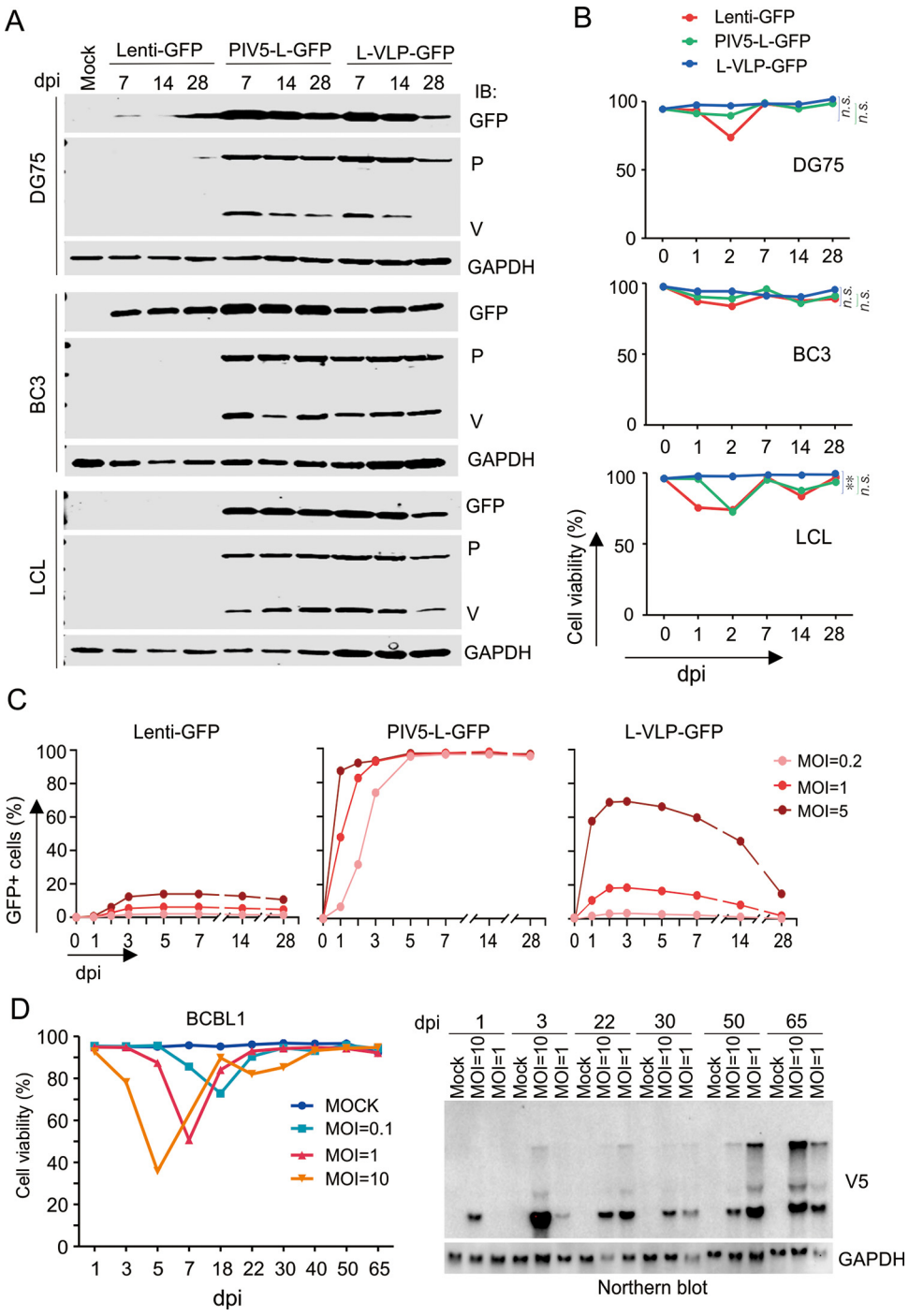

FIG 5 Persistence of different B-lymphoma cells with L-VLP infection. (A) DG75, BC3, and LCL B-lymphoma cells infected with Lenti-GFP, L-VLP-GFP, and PIV5-L-GFP (MOI, 1) after long-term culture were individually subjected to immunoblot (IB) analysis with the indicated antibodies. (B) The percentage of viable B-lymphoma cells after viral infection from panel A was quantified. **, $P < 0.05$. ns, not significant. (C) The percentage of GFP-positive LCL cells with viral infection at different MOIs after long-term culture was quantified by flow cytometry analysis. (D) Northern blot analysis of viral persistence in BCBL1 cells infected with PIV5-L (MOI of 0.1, 1, and 10) after long-term culture. The percentage of viable cells after long-term culture was quantified and is shown on the left.

deleting the HN gene and replacing the M and F genes of PIV5-L with GFP and puromycin resistance genes, respectively.

Rescue of PIV5-L-GFP particles. Briefly, we seeded 4×10^5 BHK-optT7 cells in each well of a 6-well plate and then transfected cells at 70% confluence. The amounts of the four plasmids used were 3 μg pB-PIV5-L-GFP, 1 μg pTM1-NP, 0.2 μg pTM1-P, 1.5 μg pTM1-L, and 23 μL Fugene HD. They were mixed into

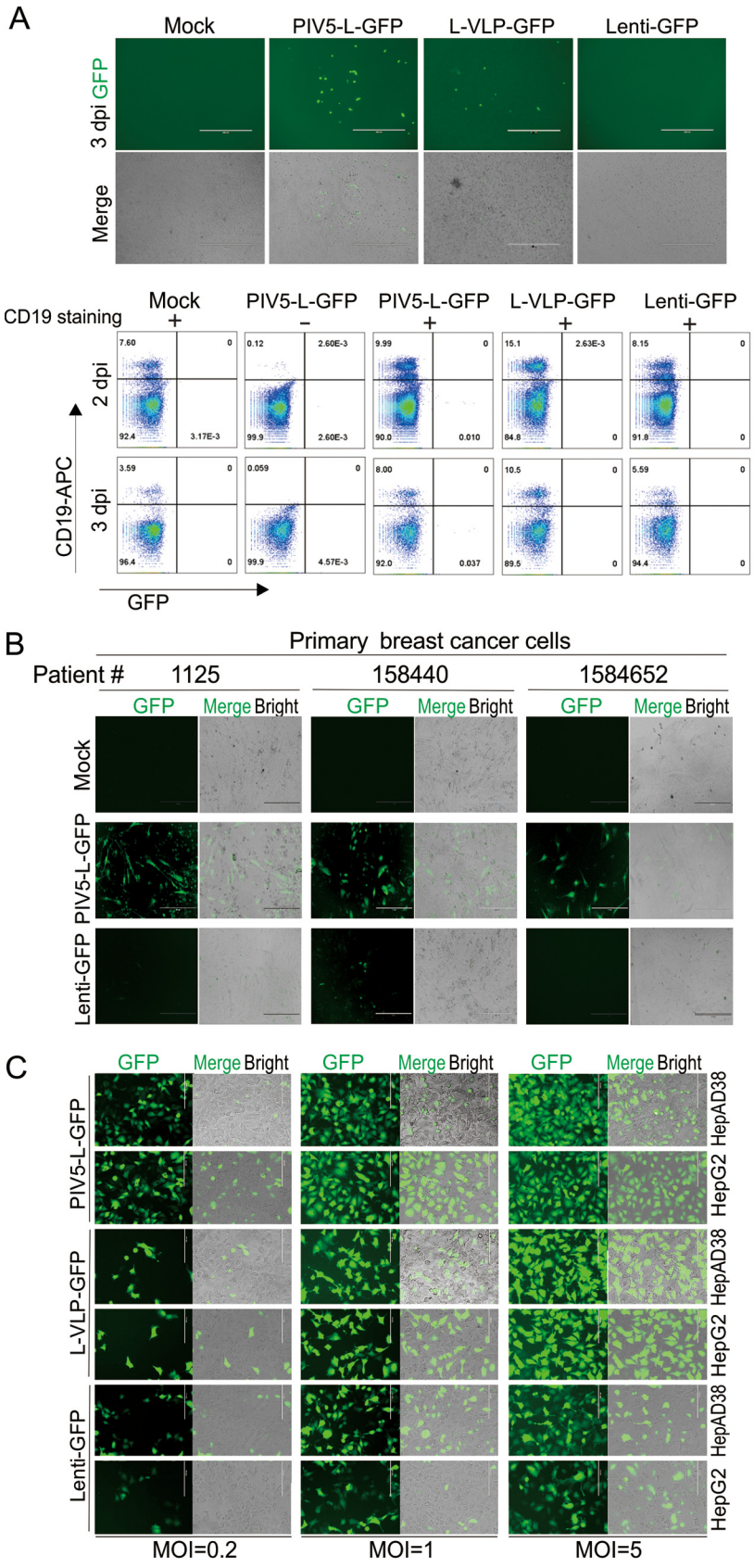

FIG 6 High infection efficiency of PIV5-L and L-VLP in primary cancer cells but not normal B cells. (A) Percentage of CD19 cells from healthy human peripheral blood mononuclear cells (PBMCs; n = 3)

(Continued on next page)

Opti-MEM with 200 μL total volume and then add to wells after incubating for 15 min at room temperature. Culture was done at 37°C without exchanging the growth medium. At 4 days posttransfection, we harvested supernatants with spinning at 3,500 rpm at 4°C for 15 min and aliquoted them for storage at −80°C for use.

Production of L-VLP-GFP particles. BHK-optT7 cells were seeded into a 6-well plate (4×10^5 per well) the day before transfection. When cells reached about 70% confluence, all plasmids, including pB-PIV5-L-VLP-GFP (2 μg), pTMI-NP (0.5 μg), pTMI-P (0.1 μg), pTMI-L (0.8 μg), pCAGGS-F (0.8 μg), pCAGGS-HN (0.8 μg), and pCAGGS-M (0.5 μg), were transfected into BHK-optT7 in one step using jetOPTIMUS transfection reagent. At 2 days posttransfection, the supernatants were collected by centrifuging at 3,500 rpm for 10 min and then aliquoted and stored at −80°C for use.

Production of lentivirus-GFP particles. pLenti-CMV-EGFP-Hygro, pVSV-G, and pSPAX2 were cotransfected into 293T cells by using polyethyleneimine (PEI) at a ratio of 4:3:1 to generate lentivirus-GFP virus particles. At 2 days posttransfection, the supernatants were collected by centrifugation at 3,000 rpm for 10 min, passed through a 0.45-μm PES filter to further remove the cell debris, and then aliquoted and stored at −80°C for use.

Quantification of L-VLP–GFP and lentivirus-GFP virus titers. To determine the L-VLP particle titer, Vero cells were seeded on the 24-well plates at 4×10^5 per well 4 h before infection. L-VLP was serially 10-fold diluted in 2% FBS–DMEM to infect Vero cells. At 2 h postinfection, culture medium was replaced with 6% FBS–DMEM. One day postinfection, cells were collected and the GFP-positive cells were detected by flow cytometry. The process of lentivirus-GFP quantification was the same as that for L-VLP. We just replaced Vero cells with 293T cells and counted them 72 h after transduction. Virus titers [Transducing Unite (TU)/milliliter] were calculated in cultures with 5% to 20% GFP-expressing cells according to the following formula: (% GFP-expressing cells/100) $\times$ number of cells at moment of transduction $\times$ dilution factor/volume of viral supernatant used for transduction (milliliters) (24). The flow data were analyzed by FlowJo v.10.

Lentivirus, PIV5-L, or L-VLP infection of cells. Adherent cells were seeded 24 h before infection. After infection, the culture medium was removed and lentivirus, PIV5-L, or L-VLP diluted in 2% FBS-DMEM at the indicated MOI was added. For cells in suspension, the culture medium was removed by centrifugation at 1,200 rpm for 4 min, and lentivirus, PIV5-L, or L-VLP diluted in 2% FBS RPMI at the indicated MOIs was added. Two hours after incubation, the inoculum was replaced with complete cell culture medium.

Single-step growth rate. Monolayers of Vero cells in 24-well plates were washed with PBS and then infected with PIV5-L in DMEM–2% FBS at an MOI of 0.1 PFU/cell for 2 h at 37°C. The cells were then maintained in DMEM–2% FBS. Medium was collected at 12, 24, 48, 72, and 96 h postinfection (hpi). The titers of viruses were determined by focus-forming assay on Vero cells.

Focus-forming assay. Vero cells were seeded in a 96-well plate (4×10^4 cells/well) 1 day before infection. When cells achieve 100% confluence, we added 100 μL/well 10-fold serially diluted virus (diluted in 2% FBS–DMEM) to cells, incubated them at 37°C for 2 h, and overlaid 125 μL of 2$\times$ DMEM containing 1% methylcellulose and 2% FBS into each well. We fixed cells with 4% paraformaldehyde (100 μL/well) at room temperature for 40 min at 3 days postincubation. The flick-off overlay was then washed with 150 μL/well blocking buffer (PBS containing 1% FBS and 0.02% Triton X-100) three times and immunostained with rabbit anti-V5 antibody (number 13202; CST) followed by horseradish peroxidase-conjugated anti-rabbit antibody. The foci were developed using TrueBlue peroxidase substrate (Sera Care) (25).

Flow cytometry analysis of PBMCs. Human PBMCs were isolated by Ficoll Paque plus (GE Healthcare). After washing with PBS, PBMCs were left uninfected (mock) or were infected with PIV5-L-GFP, L-VLP-GFP, or Lenti-GFP at an MOI of 1. At indicated times postinfection, 2×10^6 cells were harvested and stained with 50 μL of allophycocyanin mouse anti-human CD19 antibody (HIB19, 302212; BioLegend) diluted in fluorescence-activated cell sorting (FACS) buffer (PBS plus 2% bovine serum albumin and 2 mM EDTA). After incubation at 4°C in the dark for 30 min, the cells were washed once with 800 μL of cold FACS buffer. The cells were resuspended in 400 μL of FACS buffer. The stained cells were analyzed using flow cytometry. Data were analyzed using FlowJo.

Immunoblotting. Cells were harvested, washed twice with ice-cold PBS, and lysed in ice-cold radioimmunoprecipitation assay buffer (150 mM NaCl, 50 mM Tris [pH 7.6], 1% Nonidet P-40, 2 mM EDTA, proteinase inhibitor mixture [1 mM phenylmethylsulfonyl fluorine, 1 g/mL aprotinin, 1 g/mL leupeptin, and 1 g/mL pepstatin]) for 30 min on ice with brief vortexing every 5 min. The lysates were centrifuged at 14,500 rpm for 5 min at 4°C to remove cell debris. We transferred supernatant into a new tube, and the concentration of protein was determined by the Bradford method. Supernatants were boiled in 6$\times$ SDS loading buffer. Proteins were separated by SDS-PAGE and transferred to 0.45-μm nitrocellulose membrane for immunoblotting with primary antibodies and appropriate secondary antibodies. The membrane was scanned and analyzed with an Odyssey infrared scanner (Li-Cor Biosciences) (26).

Cell viability assay. The percentages of human B-lymphoma cells with or without PIV5-L infection were determined using Vi-cell XR (Beckman coulter) at different time points.

Statistical analysis. Data are presented as means $\pm$ standard deviations from two biologically independent replicates. Statistical analysis was performed using unpaired two-tailed Student's *t* tests with

FIG 6 Legend (Continued)
infected with PIV5-L-GFP, L-VLP-GFP, or Lenti-GFP at an MOI of 1 as determined by flow cytometry analysis. Representative green fluorescence images of uninfected (mock) or infected PBMCs are shown at the top. (B) Representative green fluorescence images of human primary breast cancer cells (n = 3) uninfected (mock) or infected with PIV5-L-GFP or Lenti-GFP at an MOI of 1 after 2 days. (C) Representative green fluorescence images of human liver cancer cell lines HepG2 and HepAD38 infected with PIV5-L-GFP, L-VLP-GFP, or Lenti-GFP at different MOI after 2 days.

GraphPad Prism 8.0.2. *P* values of ≤0.05 were considered statistically significant (***, $P < 0.001$; ****, $P < 0.0001$).

Data availability. Genomic sequence data generated in this study have been deposited in GenBank under accession number MT160087.

ACKNOWLEDGMENTS

This work was supported by the National Natural Science Foundation of China (81971930, 32120103001, 82102386, and 81772166), the National Key Research and Development Program (2021YFA1300803), and the Jinan University and Institute Innovation Program (2020GXRC043). Q.C. is a scholar of New Century Excellent Talents at the University of China.

REFERENCES

1. Jiang M, Bennani NN, Feldman AL. 2017. Lymphoma classification update: T-cell lymphomas, Hodgkin lymphomas, and histiocytic/dendritic cell neoplasms. Expert Rev Hematol 10:239–249. https://doi.org/10.1080/17474086.2017.1281122.
2. Jiang M, Bennani NN, Feldman AL. 2017. Lymphoma classification update: B-cell non-Hodgkin lymphomas. Expert Rev Hematol 10:405–415. https://doi.org/10.1080/17474086.2017.1318053.
3. Teras LR, DeSantis CE, Cerhan JR, Morton LM, Jemal A, Flowers CR. 2016. 2016 US lymphoid malignancy statistics by World Health Organization subtypes. CA Cancer J Clin 66:443–459. https://doi.org/10.3322/caac.21357.
4. Nicolae A, Pittaluga S, Abdullah S, Steinberg SM, Pham TA, Davies-Hill T, Xi L, Raffeld M, Jaffe ES. 2015. EBV-positive large B-cell lymphomas in young patients: a nodal lymphoma with evidence for a tolerogenic immune environment. Blood 126:863–872. https://doi.org/10.1182/blood-2015-02-630632.
5. Cesarman E. 2011. Gammaherpesvirus and lymphoproliferative disorders in immunocompromised patients. Cancer Lett 305:163–174. https://doi.org/10.1016/j.canlet.2011.03.003.
6. Yang Z, Allen CDC. 2018. Expression of exogenous genes in murine primary B Cells and B cell lines using retroviral vectors. Methods Mol Biol 1707:39–49. https://doi.org/10.1007/978-1-4939-7474-0_3.
7. Hull RN, M J, Smith JW. 1956. New viral agents recovered from tissue cultures of monkey kidney cells. I. Origin and properties of cytopathogenic agents S.V.1, S.V.2, S.V.4, S.V.5, S.V.6, S.V.11, S.V.12 and S.V.15. Am J Hyg 63:204–215.
8. Thomas SM, Lamb RA, Paterson RG. 1988. Two mRNAs that differ by two nontemplated nucleotides encode the amino coterminal proteins P and V of the paramyxovirus SV5. Cell 54:891–902. https://doi.org/10.1016/s0092-8674(88)91285-8.
9. Alayyoubi M, Leser GP, Kors CA, Lamb RA. 2015. Structure of the paramyxovirus parainfluenza virus 5 nucleoprotein-RNA complex. Proc Natl Acad Sci U S A 112:E1792–E1799. https://doi.org/10.1073/pnas.1503941112.
10. Schmitt AP, Leser GP, Waning DL, Lamb RA. 2002. Requirements for budding of paramyxovirus simian virus 5 virus-like particles. J Virol 76:3952–3964. https://doi.org/10.1128/jvi.76.8.3952-3964.2002.
11. El Najjar F, Schmitt AP, Dutch RE. 2014. Paramyxovirus glycoprotein incorporation, assembly and budding: a three way dance for infectious particle production. Viruses 6:3019–3054. https://doi.org/10.3390/v6083019.
12. Schmitt PT, Ray G, Schmitt AP. 2010. The C-terminal end of parainfluenza virus 5 NP protein is important for virus-like particle production and M-NP protein interaction. J Virol 84:12810–12823. https://doi.org/10.1128/JVI.01885-10.
13. Waning DL, Schmitt AP, Leser GP, Lamb RA. 2002. Roles for the cytoplasmic tails of the fusion and hemagglutinin-neuraminidase proteins in budding of the paramyxovirus simian virus 5. J Virol 76:9284–9297. https://doi.org/10.1128/jvi.76.18.9284-9297.2002.
14. Jardetzky TS, Lamb RA. 2014. Activation of paramyxovirus membrane fusion and virus entry. Curr Opin Virol 5:24–33. https://doi.org/10.1016/j.coviro.2014.01.005.
15. Wei H, Chen Z, Elson A, Li Z, Abraham M, Phan S, Kristhnamurthy S, McCray PB, Jr, Andrews S, Stice S, Sakamoto K, Jones C, Tompkins SM, He B. 2017. Developing a platform system for gene delivery: amplifying virus-like particles (AVLP) as an influenza vaccine. NPJ Vaccines 2:32. https://doi.org/10.1038/s41541-017-0031-7.
16. Chen Z. 2018. Parainfluenza virus 5-vectored vaccines against human and animal infectious diseases. Rev Med Virol 28:e1965. https://doi.org/10.1002/rmv.1965.
17. He B, Paterson RG, Ward CD, Lamb RA. 1997. Recovery of infectious SV5 from cloned DNA and expression of a foreign gene. Virology 237:249–260. https://doi.org/10.1006/viro.1997.8801.
18. Li K, Li Z, Wohlford-Lenane C, Meyerholz DK, Channappanavar R, An D, Perlman S, McCray PB, Jr, He B. 2020. Single-dose, intranasal immunization with recombinant parainfluenza virus 5 expressing middle east respiratory syndrome coronavirus (MERS-CoV) spike protein protects mice from fatal MERS-CoV infection. mBio 11:e00554-20. https://doi.org/10.1128/mBio.00554-20.
19. An D, Li K, Rowe DK, Diaz MCH, Griffin EF, Beavis AC, Johnson SK, Padykula I, Jones CA, Briggs K, Li G, Lin Y, Huang J, Mousa J, Brindley M, Sakamoto K, Meyerholz DK, McCray PB, Jr, Tompkins SM, He B. 2021. Protection of K18-hACE2 mice and ferrets against SARS-CoV-2 challenge by a single-dose mucosal immunization with a parainfluenza virus 5-based COVID-19 vaccine. Sci Adv 7:eabi5246. https://doi.org/10.1126/sciadv.abi5246.
20. Dillon PJ, Wansley EK, Young VA, Alexander-Miller MA, Parks GD. 2006. Exchange of P/V genes between two non-cytopathic simian virus 5 variants results in a recombinant virus that kills cells through death pathways that are sensitive to caspase inhibitors. J Gen Virol 87:3643–3648. https://doi.org/10.1099/vir.0.82242-0.
21. Wignall-Fleming EB, Hughes DJ, Vattipally S, Modha S, Goodbourn S, Davison AJ, Randall RE. 2019. Analysis of paramyxovirus transcription and replication by high-throughput sequencing. J Virol 93:e00571-19. https://doi.org/10.1128/JVI.00571-19.
22. Li Z, Gabbard JD, Mooney A, Gao X, Chen Z, Place RJ, Tompkins SM, He B. 2013. Single-dose vaccination of a recombinant parainfluenza virus 5 expressing NP from H5N1 virus provides broad immunity against influenza A viruses. J Virol 87:5985–5993. https://doi.org/10.1128/JVI.00120-13.
23. Panthi S, Schmitt PT, Lorenz FJ, Stanfield BA, Schmitt AP. 2021. Paramyxovirus-like particles as protein delivery vehicles. J Virol 95:e0103021. https://doi.org/10.1128/JVI.01030-21.
24. Vermeire J, Naessens E, Vanderstraeten H, Landi A, Iannucci V, Van Nuffel A, Taghon T, Pizzato M, Verhasselt B. 2012. Quantification of reverse transcriptase activity by real-time PCR as a fast and accurate method for titration of HIV, lenti- and retroviral vectors. PLoS One 7:e50859. https://doi.org/10.1371/journal.pone.0050859.
25. Brien JD, Lazear HM, Diamond MS. 2013. Propagation, quantification, detection, and storage of West Nile virus. Curr Protoc Microbiol 31:15d.3.1–15d.3.18.
26. Wan C, Tai J, Zhang J, Guo Y, Zhu Q, Ling D, Gu F, Gan J, Zhu C, Wang Y, Liu S, Wei F, Cai Q. 2019. Silver nanoparticles selectively induce human oncogenic gamma-herpesvirus-related cancer cell death through reactivating viral lytic replication. Cell Death Dis 10:392. https://doi.org/10.1038/s41419-019-1624-z.